Oct 17th, 12:00 AM

Non-linear Buckling Analysis of Thin-walled Metal Columns

C. Jiang

J. Michael Davies

Thirteenth International Specialty Conference on Cold-Formed Steel Structures
St. Louis, Missouri U.S.A., October 17-18, 1996

NON-LINEAR BUCKLING ANALYSIS OF THIN-WALLED METAL COLUMNS

J M Davies* and C Jiang**

Introduction

Uniformly compressed cold-formed metal columns are susceptible to instability in a variety of modes. In the stability analysis of such a column, using any of the available numerical methods with the exception of the eigenvalue method, the perfect geometry of the column must be 'seeded' with an imperfection in order to cause it to collapse. If the member buckles in a global mode, it is easy to introduce an appropriate imperfection in form of a suitable displaced shape. However, it is more difficult to define the imperfections for the distortional and local buckling modes due to the unknown nature of the critical buckling patterns.

The eigenvalue method can be used to predict the bifurcation buckling of a perfect member and linear solutions of eigenvalue problems have been well developed and documented. However, because many members buckle in the nonlinear region, it is necessary to develop non-linear solutions for eigenvalues. In the authors' studies, the eigenvectors from linear eigen-solutions have been introduced as the imperfections in non-linear finite element analysis using ABAQUS version 5.4. However, this may not always be sufficiently accurate because the patterns of linear buckling and non-linear buckling could be different.

Unfortunately, if a problem with a large number of degrees of freedom is analyzed using the finite element method, the existing methods are expensive in terms of either time or memory consumption. In this paper, a non-linear solution of eigenvalue problems set up using the finite element method is developed. The method has been used to analyze some stability problems in the uniformly compressed uprights of steel pallet racks. The results from analyses and tests agree well [1].

Geometric and material non-linearity

It is well known that geometric non-linearity in degenerate shell elements is caused by the second strain derivative terms [2]:

* Professor of Structural Engineering ** Research Fellow
Manchester School of Engineering, University of Manchester, Manchester, U.K

$$\boldsymbol{\varepsilon} = \begin{bmatrix} \varepsilon_{x'} \\ \varepsilon_{y'} \\ \gamma_{x'y'} \\ \gamma_{x'z'} \\ \gamma_{y'z'} \end{bmatrix} + \begin{bmatrix} \dfrac{\partial u'}{\partial x'} \\ \dfrac{\partial v'}{\partial y'} \\ \dfrac{\partial u'}{\partial y'} + \dfrac{\partial v'}{\partial x'} \\ \dfrac{\partial u'}{\partial z'} + \dfrac{\partial w'}{\partial x'} \\ \dfrac{\partial v'}{\partial z'} + \dfrac{\partial w'}{\partial y'} \end{bmatrix} + \begin{bmatrix} \dfrac{1}{2}\left(\dfrac{\partial w'}{\partial x'}\right)^2 \\ \dfrac{1}{2}\left(\dfrac{\partial w'}{\partial y'}\right)^2 \\ \dfrac{\partial w'}{\partial x'}\dfrac{\partial w'}{\partial y'} \\ 0 \\ 0 \end{bmatrix} = \boldsymbol{\varepsilon}_e + \boldsymbol{\varepsilon}_l \qquad (1)$$

where u′, v′ and w′ are displacement components in the direction of the local cartesian coordinates x′, y′ and z′ of the element and ϵ_e and ϵ_l are respectively the linear and the non-linear contributions to the strains. The bold symbols denote matrices and column vectors. Material non-linearity may be considered as [2]:

$$d\boldsymbol{\sigma} = \mathbf{D}_{ep}\, d\boldsymbol{\varepsilon} \qquad (2)$$

with the elastic-plastic matrix $\mathbf{D}_{ep}$ given by:

$$\mathbf{D}_{ep} = \mathbf{D} - \frac{\mathbf{D}\,\mathbf{a}\,\mathbf{a}^T\mathbf{D}}{H' + \mathbf{a}^T\mathbf{D}\,\mathbf{a}} \qquad (3)$$

In the above equations, $\boldsymbol{\sigma}$ and $\boldsymbol{\epsilon}$ are the stress and strain vectors respectively, **D** is the general elasticity matrix, **a** is the general displacement vector and H′ is the hardening parameter. These non-linearities are considered in forming the stiffness matrix **K** and the geometric stiffness matrix $\mathbf{K}_g$.

Non-linear eigenvalue problems

In finite element analysis, the second-order behaviour of a structure can be expressed by the following equation

$$(\mathbf{K} + \mathbf{K}_g)\,\mathbf{a} = \mathbf{F} \qquad (4)$$

The geometric stiffness matrix $\mathbf{K}_g$ depends on the stresses $\boldsymbol{\sigma}$ caused by the external forces **F**. In both linear and non-linear stability analyses, the applied load on the structure is regarded as a fixed loading pattern multiplied by some factor λ. The critical load vector $\mathbf{F}_{cr}$ can be defined as the load **F** multiplied by the smallest value of λ at which the displacements of structure become indeterminate, i.e. at bifurcation of equilibrium. This condition can be written mathematically as:

$$(\mathbf{K} + \lambda \mathbf{K}_g)\,\mathbf{a} = \mathbf{0} \qquad (5)$$

This is a problem of determining eigenvalues λ_i and corresponding eigenvectors $\mathbf{a}_i$ (buckling patterns) for the pair of matrices $\mathbf{K}$ and $\mathbf{K}_g$.

From the engineering point of view, only the lowest value of the critical load has practical significance so that it is only necessary to determine the minimum value of λ. However, in the case when such a bifurcation has a stable character, a secondary critical load may be of importance. This is a consequence of the differences between perfect structures and imperfect structures.

In a linear stability analysis, the matrix $\mathbf{K}$ of equation (5) is the global elastic stiffness matrix $\mathbf{K}_e$ which is independent of the stress and strain levels and $\mathbf{K}_g$ is independent of the load history. For a nonlinear buckling analysis, the matrix $\mathbf{K}$ in equation (5) has to be the global elastic-plastic matrix $\mathbf{K}_{ep}$. In this case, the matrix $\mathbf{K}_{ep}$ is not constant because the plastic property matrix depends on the stress level and specific features of the material models. Furthermore, $\mathbf{K}_g$ is then dependant on the stress-strain history.

Existing non-linear solutions of eigenvalue problems

Non-linear solutions of equation (5) can be achieved by an appropriate modification of the elasto-plastic stiffness matrices $\mathbf{K}_{ep}$ and $\mathbf{K}_g$ at each load increment, so as to include suitable stress-dependent coefficients that are representative of the state of plasticity in the material.

For non-linear buckling analysis, the critical state of stress is reached when λ in equation (5) is equal to unity. One way of solving this problem is the method adopted by Pifko and Isakson [3], in which a process of trial and error was used employing a bisection strategy. In this method, the stress state is calculated, the matrices $\mathbf{K}_{ep}$ and $\mathbf{K}_g$ are then computed based on these stresses at a trial loading level, and the corresponding lowest eigenvalue is then determined. If the eigenvalue so determined is sufficiently close to one, then the trial loading is critical. If it does not equal one, the current trial loading has to be increased or decreased for the next trial. This procedure is repeated until λ equals one or the convergence criterion is satisfied. Obviously, this method is simple and easy to programme. However, it is rather inefficient because it involves repeatedly solving the eigenvalue problem at every trial loading level.

Gupta presented a method [4-6] which was based on the Sturm sequence property [7,8] also employing the bisection strategy. The most useful consequence of the Sturm sequence property is that for any guessed value of λ, the number of sign changes in the determinant of $(\mathbf{P}_i - \lambda\mathbf{I})$ for $i = 0, 1, 2, \ldots n$ is equal to the number of eigenvalues of $(\mathbf{P} - \lambda\mathbf{I})$ which are less than λ. The matrix $\mathbf{I}$ is the unit matrix and the matrix $\mathbf{P}$ results from the standard form

$$(\mathbf{P} - \lambda\,\mathbf{I})\,\mathbf{x} = \mathbf{0} \qquad (6)$$

of the general eigenvalue equation (5). Gupta's method avoids the computation of the eigenvalue at each trial loading level which makes the method more efficient. However, the

method involves a triangularization process at each trial load level and needs core to store the upper symmetric half of both of the matrices $\mathbf{K}_{ep}$ and $\mathbf{K}_g$. When a problem with a large number of degrees of freedom is dealt with, much memory and computation time are consumed. This method was used by Lau and Hancock in combination with the spline finite strip method [9].

An improved solution for eigenvalues

The method proposed in this paper [1] is based on the inverse shift iteration technique in combination with a finite element analysis using degenerate shell elements.

The stiffness matrix $\mathbf{K}_{ep}$ can be obtained from the normal procedures for stress analysis using the finite element method. The geometrical stiffness matrix $\mathbf{K}_g$ depends on the values of the stresses in the elements as well as on the assumed displacement field. In special cases, the stresses in the elements may be known exactly. However, this is usually not usually the case so that a stress analysis by the finite element method, using the same element discretization as the subsequent buckling analysis, seems natural.

Since an iteration scheme is used to solve a nonlinear problem, the load is gradually increased by increasing the load factor Λ. If the inverse shift iteration technique is used to compute the eigenvalue, the lowest eigenvalue λ_i can be always obtained at each load level (Λ_i should be kept small in order to prevent the load from reaching the higher buckling modes). Based on the eigenvalue λ_i at the last load level, the current load factor Λ_{i+1} can be predicted to make the current eigenvalue equal one. The load factor Λ_{i+1} for next eigenvalue solution is then suggested as:

$$\Lambda_{i+1} \geq \Lambda_i + \eta\left(\lambda_i - 1\right) \quad \text{if } \lambda_i > 1 \tag{7}$$

$$\Lambda_{i+1} \leq \Lambda_i + \eta\left(\lambda_i - 1\right) \quad \text{if } \lambda_i < 1 \tag{8}$$

where the factor η $(0 < \eta < 1)$ can affect the convergence speed of the eigenvalue solution. The optimum value of η depends on the problem being analyzed and the 'gold division coefficient' 0.618 is suggested for general use.

Figure 1 is the flow-chart that shows how the subroutine is connected to a programme of normal stress analysis.

Optimization of the computation

If. a normal solution method is adopted to solve equation (5), for example the Gaussian elimination method, for a relatively simple problem with (say) 150 nodes using a PC-486DX with a 6.75-megabyte memory, many hours of computation would be needed. It follows that it is practically impossible to analyze stability problems of this type on a PC with a normal equation solution method. However, the matrix $\mathbf{K}_{ep}$ is symmetrical and its coefficients have a 'banded' structure as shown in Figure 2.

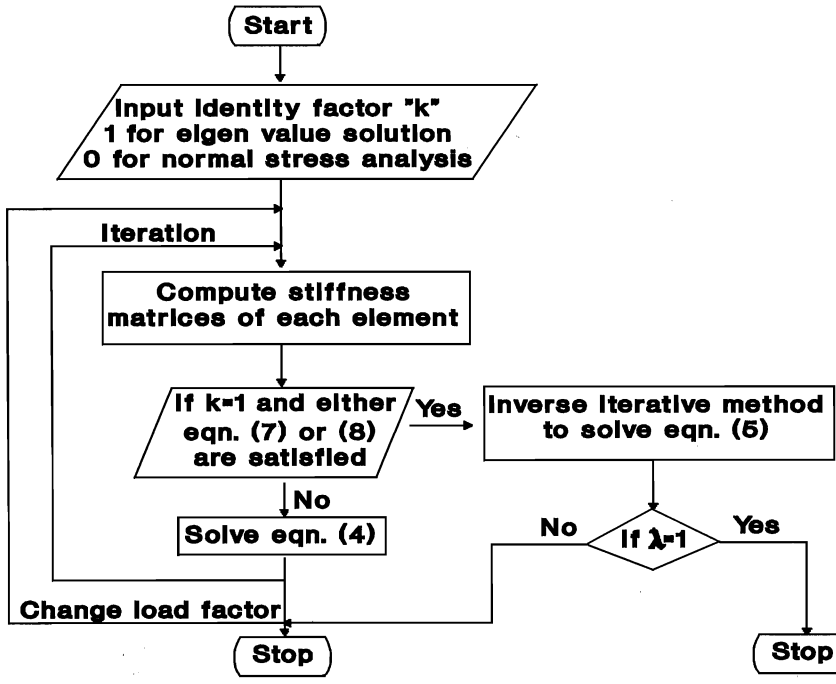

Figure 1 Flow-chart for improved eigenvalue solution

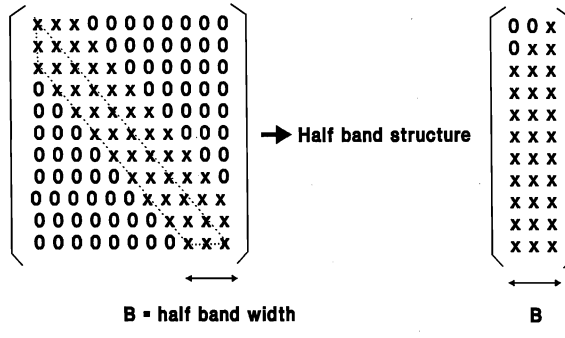

Figure 2 Banded structure of a typical finite element analysis

This means that the coefficients are clustered around the diagonal stretching from the top left hand corner of the matrix $\mathbf{K}_{ep}$ to the bottom right-hand corner. In this case, there are never more than B non-zero coefficients on either side of the leading diagonal in any row, where

B is the half band width:

$$B = (d + 1)f \tag{9}$$

where d is the maximum difference in the node numbers for all of the elements of the assemblage and f is the number of degrees of freedom at each node. Since the displacements u, v and w of the ninth node of the 9-node Heterosis element used in the authors' analysis are restrained, the half band width B for this case is:

$$B = (d + 1)f - 3 \tag{10}$$

Therefore, only the leading diagonal terms and B - 1 additional coefficients per row need to be stored for calculation and a great deal of memory and computation time can be saved. The most economical method of storage is to store the lower band of the matrix in a rectangular array by shifting the rows in order to align the band structure. With this half banded array, equation (5) for the typical problem discussed above can be solved by Cholesky's method [7] using only 0.786 megabytes of memory and about 5 minutes computation time.

It may be noted that, in each iteration i, $\mathbf{K}_g\mathbf{a}_i = \mathbf{a}_{i+1}$ has to be computed and $\mathbf{K}_g$ is a very large array. In order to save further memory, an efficient method is to compute $\mathbf{k}_g\mathbf{a}_i$ for each element and to add the products to $\mathbf{a}_{i+1}$ simultaneously without assembling and storing $\mathbf{K}_g$.

In practice, at each load level, the nodal displacements are substituted for the eigenvector **a**, instead of an identity vector as generally adopted in equation (5), in order to accelerate convergence. By this method, for a problem which will be described later, the estimated eigenvalue could be obtained with only 20 iterations while, if the identity vector is used, more than 70 iterations would be needed in order to achieve the same accuracy in the estimated eigenvalue. The computer codes for the developed method can be found in reference [1].

Analyses of uniformly compressed columns

A total of 68 channel sections of different sizes and shapes, thicknesses and steel grades were tested in the fixed-ended condition under uniform compression by Lau and Hancock [9] and analyzed using the finite strip method. These sections and lengths are typical of those used in practical pallet rack construction. The sections RA17, RA24, RL17 and RL24, as shown in Figure 3, have been analyzed using the developed method with 9-node Heterosis shell elements.

The mean stress-strain curves of HR340 and G450 steel from which the columns were made, as shown in Figures 4(a) and (b), were determined from tests. These were assumed to be reasonably representative for the specimen material and therefore they were used by Lau and Hancock in their inelastic finite strip analysis. The nonlinear range of the stress-strain curves is highly significant since the majority of members failed in this range. Because of the cold-forming operation, strain hardening and age hardening would be caused at the corners of the member and these should be taken into account in the analysis. Figures 4(a) and (b) show

the mean stress-strain curves obtained by tests and these were reduced to analytical curves for inclusion in the analysis.

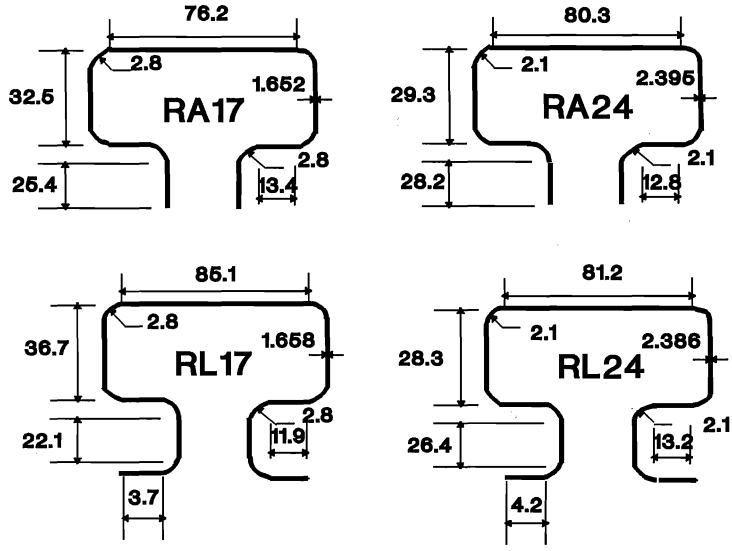

Figure 3 Dimensions of sections RA17, RA24, RL17 and RL24

An analysis to evaluate the accuracy of the Heterosis element mesh was performed for the RA24-300 section (the suffix 300 is the specimen length in mm). The two meshes used are shown in Figure 5(a) for 18 x 15 elements and in Figure 5(b) for 14 x 8 elements and the resulting buckling stresses may be compared. It was found that the mesh shown in Figure 5(b) is sufficiently accurate and that the buckling stress computed with this arrangement is only approximately 2.6% higher than is obtained using the more refined mesh shown in Figure 5(a). In order to economise on computation, 14 x (L/34) elements, where L is the length of the member, were adopted in the authors' analyses. The maximum aspect ratio of the length b to the thickness t of the elements was less than 18.5.

Results and comparison with tests

The results given by a number of alternative analyses, such as the finite element method (FEM) with the developed eigenvalue method, the 'Generalized Beam Theory' (GBT) [10] and the spline finite strip method (SSM) [9] are compared with the test results in Figures 6-9 and in the Appendix. The subscript 'in' donates the nonlinear analysis and F_y is the yield stress of the material. A typical buckling configuration, which is plotted from the computed eigenvectors obtained using FEM, is shown in Figure 10.

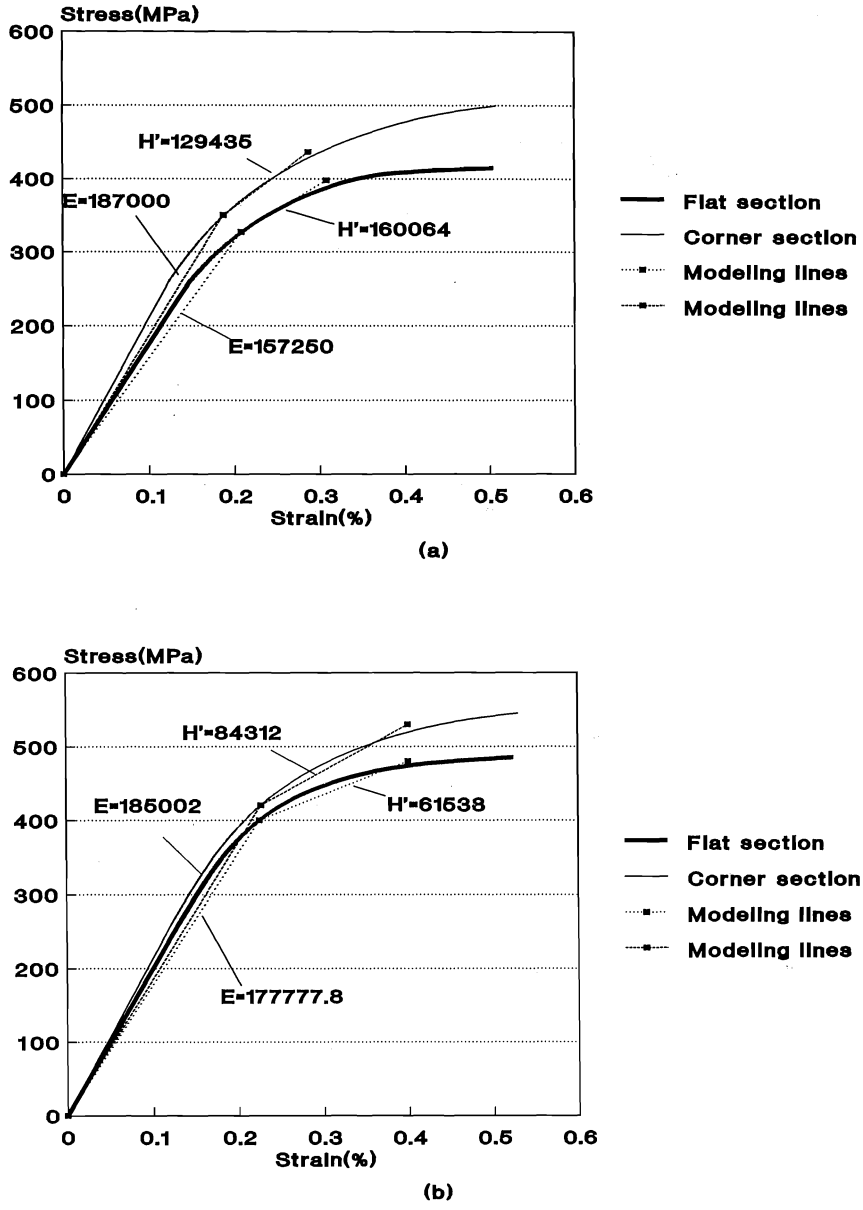

Figure 4 Mean stress-strain curves (a) HR340 steel (b) G450 steel

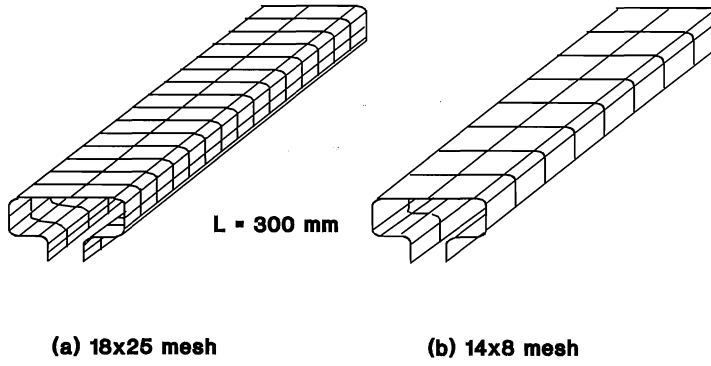

Figure 5 Two mesh options for finite element analysis

It is interesting to note the following phenomena:

1. The buckling mode given by FEM can be different from that given by the spline finite strip method. For specimen RA17-800, both the elastic and inelastic buckling modes from the finite element method are local modes while those from the finite strip method are distortional. For RA24-1500, the inelastic buckling mode from finite element method is a flexural mode, which agrees with the test, while that predicted by the finite strip method is distortional. For these sections, the results obtained using finite strip methods are slightly lower than those using finite element methods.

2. In the non-linear analysis of the section RA24-300 using FEM, an eigenvalue λ equal to one could not be achieved. This meant that the member failed in compressive yield before buckling could occur. This case can often be met in the analysis of a stub column.

3. The wave lengths of distortional buckling of sections RA17 1300-1900 and RL17 1300-1900 are so long that the number of buckling half waves could not be determined though they are evidently much longer than those of local buckling.

4. Fixed end conditions have a great influence on torsional buckling. In the analyses using FEM, the torsional buckling mode does not appear to occur due to the boundary condition where the three displacement components u, v and w and the two rotation components α and β of nodes are restrained.

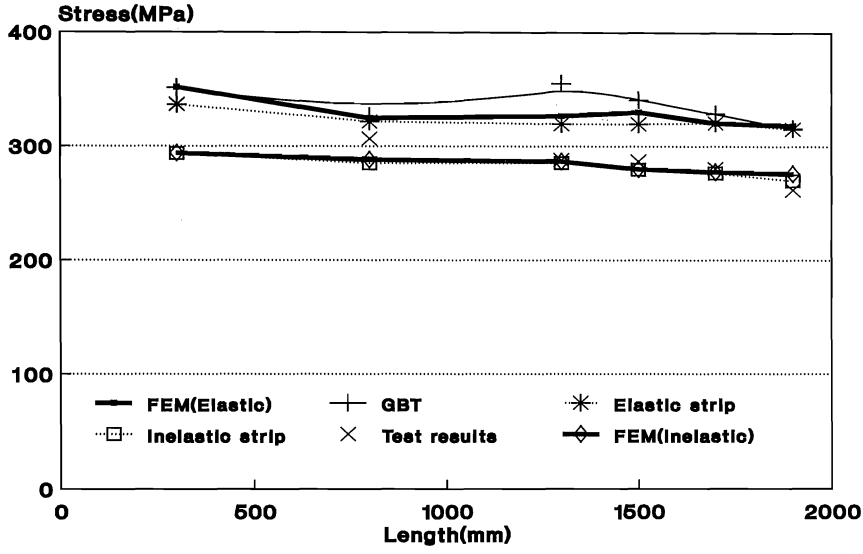

Figure 6 Theoretical and test results for RA17 section

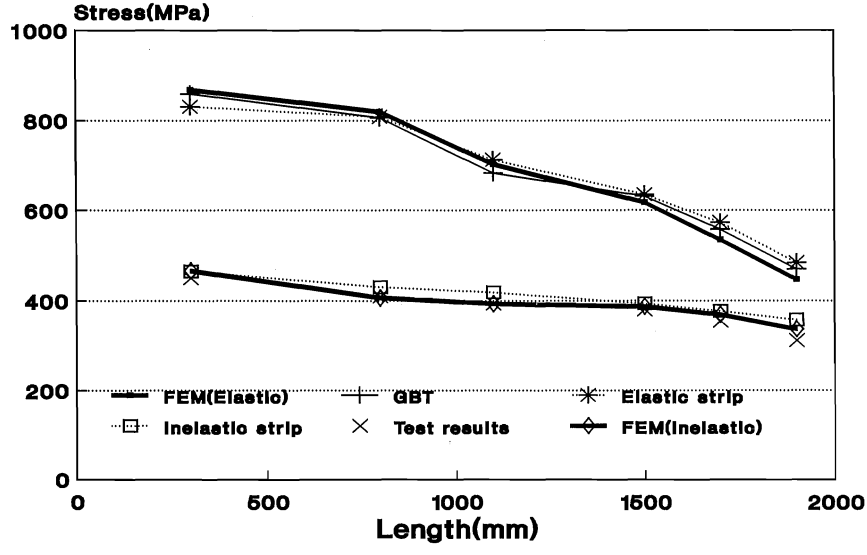

Figure 7 Theoretical and test results for RA24 section

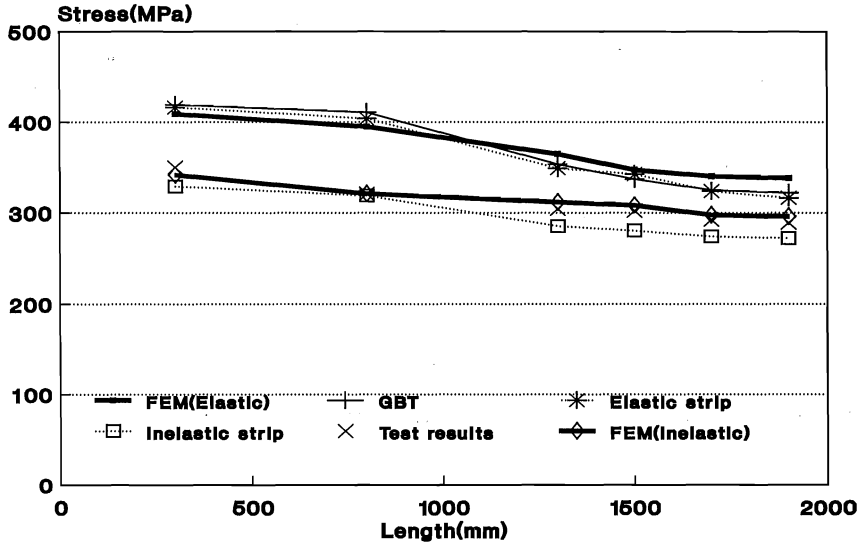

Figure 8 Theoretical and test results for RL17 section

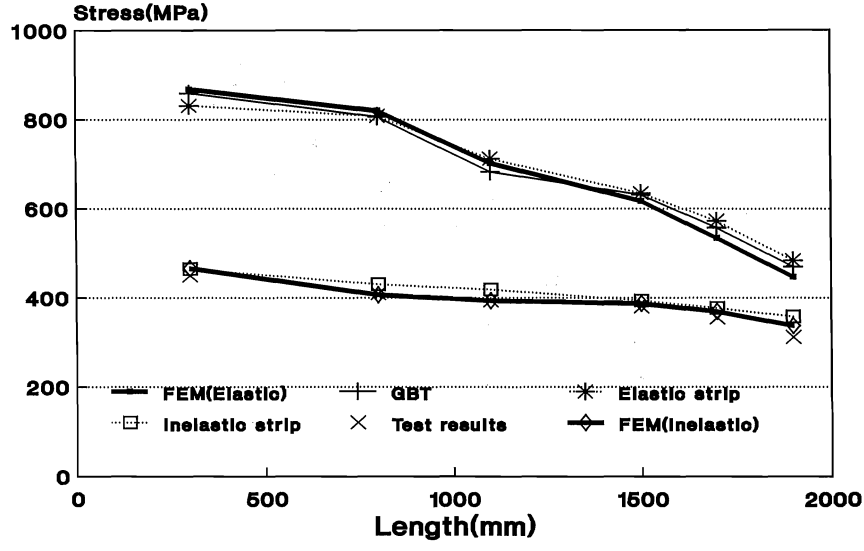

Figure 9 Theoretical and test results for RL24 section

Conclusions

The method of non-linear eigenvalue solution discussed in this paper is worthy of recognition because it produces an accurate prediction of the buckling stresses using a relatively simple procedure which requires much less memory and computing time in order to determine the eigenvalue.

The analysis used for the uniformly compressed columns is slightly more accurate for shorter wave-length local and distortional modes than for the longer wave-length flexural-torsional modes, probably as a result of geometric imperfections which would have a greater effect on the longer wave-length modes and which were not accounted for in the eigenvalue analysis. Another reason is presumably the number of elements used which can, of course, also affect the accuracy of the solution.

Greater attention should be given to the distortional buckling mode by the designers of cold-formed sections. For columns with cross-sections and lengths commonly used in practice, distortional buckling may be more critical than either local buckling or torsional flexural buckling.

It may be noted that the effect of imperfections can be great for imperfection sensitive structures and an eigenvalue solution can over estimate the maximum load capacity of a structure. In this situation, the eigenvectors from the non-linear eigen-solution may be introduced as an imperfection pattern. This method is preferred if the post-buckling behaviour is accompanied by a secondary path.

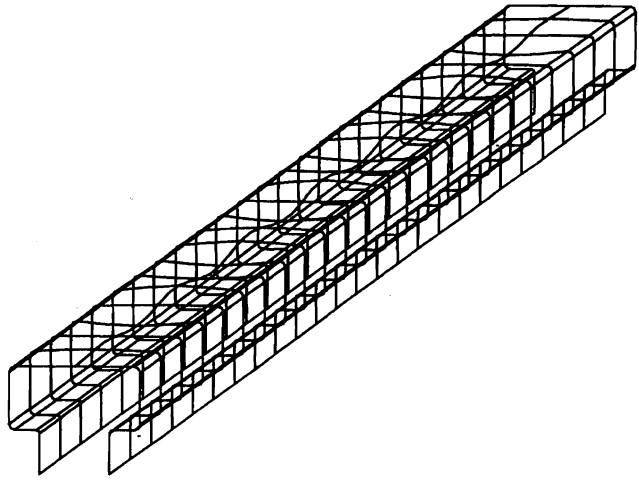

Figure 10 A typical buckling configuration obtained using FEM

References

1. Jiang C., "Stability analysis of light gauge steel members using the finite element method and the Generalised Beam Theory", PhD thesis, University of Salford, 1994.

2. Figueiras J. A. and Owen D. R. J., "Analysis of elasto-plastic and geometrically non-linear anisotropic plates and shells", eds. Hinton E. and Owen D. R. J., "Finite Element Software for Plates and Shells", Pineridge Press Ltd, 1984.

3. Pifko A. and Isakson G. " A finite element method for the plastic buckling analysis of plates", AIAA Journal, Vol. 7, No.10, 1969.

4. Gupta K. K. "Solution of eigenvalue problems by the Sturm sequence method", International Journal for Numerical Methods in Engineering, Vol. 4, 1972.

5. Gupta K. K. "Eigenproblem solution by a combined Sturm sequence and inverse iteration technique", International Journal for Numerical Methods in Engineering, Vol. 7, 1973.

6. Gupta K. K. "On a numerical solution of the plastic buckling problem of structures", International Journal for Numerical Methods in Engineering, Vol. 12, 1978.

7. Wilkinson J. H., "The Algebraic Eigenvalue Problem", Oxford University Press, London, 1965.

8. Griffiths D. V. and Smith I. M. "Numerical Methods for Engineering", Blackwell Scientific Publications, 1991.

9. Lau S. C. W. and Hancock G. J. "Inelastic buckling analysis of beams, columns and plates using the spline finite strip method", Thin-Walled Structures, 7, 1989.

10. Davies J. M. and Leach P. "Some applications of Generalised Beam Theory", Proc. 11th Int. Speciality Conf. on Cold-Formed Steel Structs., St. Louis, Missouri, October 1992.

Appendix Analytical results

Section RA17 (E = 185 kN/mm^2, F_y = 406.2 N/mm^2)

Length (mm)	SSM (MPa)	SSM_{in} (MPa)	GBT (MPa)	FEM (MPa)	FEM_{in} (MPa)	TEST (MPa)
300	416.3L	329.1 L	419.3	409.1 L	341.9 L	350.5 L
800	403.9D(1)	318.9D(1)	410.9	394.8 L	321.0 L	320.7D(1)
1300	348.9D(2)	285.4D(2)	353.5	364.7 D	311.6 D	304.3D(2)
1500	342.5D(3)	280.5D(3)	337.1	347.3 D	308.1 D	302.2D(3)
1700	323.8D(3)	274.0D(3)	324.9	340.3 D	297.6 D	292.4D(3)
1900	316.3D(3)	272.3D(3)	322.1	338.2 D	296.2 D	289.1D(3)

Section RA24 (E = 200 kN/mm^2, F_y = 478.8 N/mm^2)

Length (mm)	SSM (MPa)	SSM_{in} (MPa)	GBT (MPa)	FEM (MPa)	FEM_{in} (MPa)	TEST (MPa)
300	855.1L	457.2L	874.4	860.0L	-----	456.0L
800	661.7D(2)	407.1D(2)	650.1	652.9D(1)	416.7D	412.5D(1)
1100	577.7D(2)	399.4D(2)	593.2	596.3D(2)	393.5D	382.0D(2)
1500	534.0D(3)	391.7D(3)	551.7	588.7D(3)	392.3FT	367.0 FT
1700	528.5D(4)	383.6FT	537.5	570.8FT	389.0FT	367.0 FT
1900	519.1 FT	365.3FT	480.9	562.4FT	366.7FT	335.2 FT

Section RL17 (E = 185 kN/mm^2, F_y = 406.2 N/mm^2)

Length (mm)	SSM (MPa)	SSM_{in} (MPa)	GBT (MPa)	FEM (MPa)	FEM_{in} (MPa)	TEST (MPa)
300	336.5L	293.6L	351.3	351.8L	293.9L	337.0L
800	321.6L	287.9D(1)	326.3	324.2L	288.0L	306.5D(1)
1300	319.5D(2)	285.4D(2)	355.2	322.6D	286.6D	288.0D(2)
1500	319.5D(2)	279.7D(3)	340.7	320.0D	280.1D	286.9D(3)
1700	320.5D(3)	276.6D(3)	328.6	320.3D	277.6D	280.4D(3)
1900	315.2D(3)	269.6D(3)	315.5	318.2D	276.0D	262.0D(3)

Section RL24 (E = 200 kN/mm^2, F_y = 478.8 N/mm^2)

Length (mm)	SSM (MPa)	SSM_{in} (MPa)	GBT (MPa)	FEM (MPa)	FEM_{in} (MPa)	TEST (MPa)
300	830.8L	464.9L	867.8	857.1L	466.1L	450.5L
800	807.9L	430.2D(2)	819.4	801.8L	406.7D	410.2D(1)
1100	702.6D(2)	418.7D(2)	702.7	719.6D	393.5D	393.9D(2)
1500	645.0D(3)	393.7 FT	617.2	633.7D	386.9FT	380.0 FT
1700	572.9FT	376.8 FT	534.6	589.5FT	369.1FT	354.9 FT
1900	484.1FT	357.6 FT	447.2	502.4FT	336.7FT	311.5 FT

In the table, the numbers in parentheses are the numbers of distortional buckling half waves revealed by the analyses and:

L = local mode
D = distortional mode
FT = torsional-flexural mode